Efficient Reaching Law for SMC with PID Surface Applied to a Manipulator

Pranav
Instrumentation and Control Engineering Division
Netaji Subhas Institute of Technology,
Dwarka, New Delhi–110078, India
pranavp.kvvp@gmail.com

J. Kumar
Instrumentation and Control Engineering Division
Netaji Subhas Institute of Technology,
Dwarka, New Delhi–110078, India
singhjitendra86@gmail.com

V. Kumar
Instrumentation and Control Engineering Division
Netaji Subhas Institute of Technology,
Dwarka, New Delhi–110078, India
vineetkumar27@gmail.com

K.P.S. Rana
Instrumentation and Control Engineering Division
Netaji Subhas Institute of Technology,
Dwarka, New Delhi–110078, India
kpsranal@gmail.com

Abstract— **Robotic manipulators are employed in various applications like pick and place, painting and welding etc. In these applications it is required to track a predefined trajectory. For the same an efficient controller is required as the manipulator is a nonlinear complex and coupled system. Due to nonlinearities and coupling effect, the design of an ideal controller has been a challenging task. This paper presents a comparative study of sliding mode control (SMC) with proportional, integral, and derivative sliding surface with three different reaching laws, namely, constant rate, exponential and power rate reaching law to control a two-link robotic manipulator. All the three cases for different reaching laws are investigated for trajectory tracking, disturbance rejection and mass uncertainty. The control parameters for SMC and boundary layer are tuned with Genetic Algorithm optimization technique. Simulation results show that the power rate reaching law offers better performance than the other two laws for disturbance rejection and mass uncertainties, whereas all the three laws performed equally well for set-point tracking.**

Keywords— **Two-link robotic manipulator, Sliding mode control, Reaching law, Stability analysis, Chattering, Genetic algorithm.**

I. Introduction

Control of uncertain nonlinear systems has always been an important and popular area of research. One such system i.e. a two-link manipulator finds major applications in various industries for pick and place, welding and painting etc. For these applications even a small tracking error may lead to undesired results. Therefore, suitable controllers need to be designed for this task and various techniques have been suggested for accurate trajectory tracking and disturbance rejection of robotic manipulator.

Sliding mode control (SMC) provides robustness and invariance to uncertainties in model parameters. Many researchers have implemented SMC using conventional surface for robotic manipulator. Acob *et al.* compared conventional SMC, Proportional and Derivative (PD) controller with a hybrid combination of the two and observed that hybrid controller has greater robustness than standard SMC and PD controllers [1]. Fallaha *et al.* implemented SMC with constant rate and exponential reaching law for three degrees of freedom robotic manipulator. It was concluded that exponential rate reaching law gave better chattering and tracking performance [2]. Kuo and Huang proposed SMC with Proportional, Integral and Derivative (PID) sliding surface (SMCPID) and inferred that the PID sliding surface provided better response than the conventional PD surface [3]. Dhaval *et al.* compared conventional SMC and fuzzy based SMCPID for two-link robotic manipulator and showed that the later approach gives better performance than the former in terms of model uncertainty and external disturbances [4]. Vijay and Jena implemented SMC with adaptive PID sliding surface and adaptive PID controller and concluded that SMCPID showed favorable tracking performance and robustness with regard to disturbance in input torque [5]. One of the undesired effects in SMC, chattering, may lead to unwanted heat loss, and wear and tear in the actuator. Boundary layer was used to remove chattering and provide smoothness to the control signal as reported by Chen *et al.* [6].

Based on a brief survey presented above comparison of different reaching control laws with respect to disturbance rejection and mass uncertainty of SMCPID with two-link planar rigid robotic manipulator has not been reported and the present work is motivated from this very fact.

The remainder of this paper is divided into four sections. The mathematical model of two-link planar rigid robotic manipulator is presented in Section II, while Section III explains SMC with different reaching laws, Lyapunov stability analysis, and their implementation. Section IV presents the simulation results for trajectory tracking, disturbance rejection and mass uncertainty in detail. Lastly, Section V highlights the conclusion of proposed work.

II. Two-Link Manipulator

A two-link planar rigid robotic manipulator is considered with masses m_1 and m_2 concentrated at the end of each link as shown in Fig. 1.

The dynamic equation of two-link manipulator can be written as [7, 8]:

$$\tau = M(\theta)\ddot{\theta} + C\left(\theta,\dot{\theta}\right) + G(\theta) \quad (1)$$

where $\theta = [\theta_1 \quad \theta_2]^{\mathrm{T}}$ and $M(\theta)$ is a 2 x 2 inertial matrix, $C\left(\theta,\dot{\theta}\right)$ is a 2 x 1 matrix of centrifugal and coriolis terms, and $G(\theta)$is a 2 x 1 matrix of gravity terms.

$$\tau_1 = (m_1 + m_2){l_1}^2\ddot{\theta}_1 + m_2{l_2}^2\left(\ddot{\theta}_1 + \ddot{\theta}_2\right) + m_2 l_1 l_2\left(2\ddot{\theta}_1 + \ddot{\theta}_2\right)\cos\theta_2 - m_2 l_1 l_2\left(2\dot{\theta}_1 + \dot{\theta}_2\right)\dot{\theta}_2\sin\theta_2 + (m_1 + m_2)gl_1\cos\theta_1 + m_2\, gl_2\cos(\theta_1 + \theta_2) \quad (2)$$

$$\tau_2 = m_2{l_2}^2\left(\ddot{\theta}_1 + \ddot{\theta}_2\right) + m_2 l_1 l_2\ddot{\theta}_1\cos\theta_2 + m_2\, gl_2\cos(\theta_1 + \theta_2) + m_2\, l_1 l_2{\dot{\theta}_1}^2\sin\theta_2 \quad (3)$$

where $\theta_1$and θ_2, $\tau_1$and τ_2, $m_1$and m_2, and $l_1$and l_2 are the positions, required torques, masses and lengths of link 1 and link 2 respectively.

978-1-4673-9080-4/16/$31.00 ©2016 IEEE

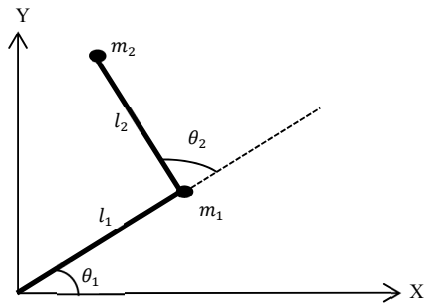

Fig. 1. Two-Link Planar Rigid Robotic Manipulator

TABLE I. PARAMETERS FOR TWO-LINK MANIPULATOR

Parameters	*Symbol*	*Values*	*Unit*
Link 1 length	l_1	0.8	m
Link 2 length	l_2	0.4	m
Link 1 mass	m_1	0.1	kg
Link 2 mass	m_2	0.1	kg
Acceleration due to gravity	g	9.8	m/s^2

The parameters for the manipulator model used in this study are described in Table I [9, 10]. Equations (2) and (3) show the relationship between controller output (τ) and link position (θ) for both links [9, 10].

III. SLIDING MODE CONTROL

SMC is a powerful control technique widely used for nonlinear multi-input multi-output systems. In SMC a control law is required to make the system states attract towards the sliding surface [11, 12]. A conventional sliding surface includes PD error term ($s(t) = \lambda e(t) + \dot{e}(t)$). An additional integral term can also be included with these terms to enhance the capability of the controller.

$$s(t) = \lambda e(t) + \dot{e}(t) + \int e(t)dt \quad (4)$$

where $e(t)$ is the error in angular position of respective links

$$e(t) = \theta_d(t) - \theta(t) \quad (5)$$

where $\theta_d(t)$ is the desired angular trajectory and $\theta(t)$ is the angular trajectory followed by respective links.

Constant rate, exponential and power rate are the three basic reaching laws widely implemented with SMC to effectively drive the system state reach equilibrium.

Constant rate reaching law can be described by (6)

$$\dot{s}(t) = -\varepsilon\, sgn\big(s(t)\big)\ \ \varepsilon > 0 \quad (6)$$

where ε is a constant. It drives the system states at a constant rate which switches at the same rate at the vicinity around the sliding surface.

Extra terms can be added in the reaching law to vary the system states to reach sliding surface. Exponential reaching law as given in (7) has $ks(t)$ as an extra term.

$$\dot{s}(t) = -\varepsilon\, sgn\big(s(t)\big) - ks(t), \varepsilon > 0, k > 0 \quad (7)$$

Hence k and ε states different rate for system states to reach sliding surface when they are far from it and when they are near to the surface.

Whereas, power rate reaching law includes a power term α as shown in (8). In this technique a high gain k increases the reaching speed, whereas α adjusts the sliding rate at the surface.

$$\dot{s}(t) = -k|s(t)|^{\alpha} sgn\big(s(t)\big), k > 0, 1 > \alpha > 0 \quad (8)$$

Apart from this a boundary layer approach is followed to reduce chattering in the controller output. Instead of $sgn\big(s(t)\big)$, $sat\big(s(t)\big)$ is used such that switching from -1 to 1 or vice versa is followed through a linear path. This makes the switching action continuous and thus reduces chattering.

$$sat\big(s(t)\big) = \begin{cases} 1, & s > \Delta \\ ks, & |s| \le \Delta \ \text{ and } k = 1/\Delta \\ -1, & s < -\Delta \end{cases} \quad (9)$$

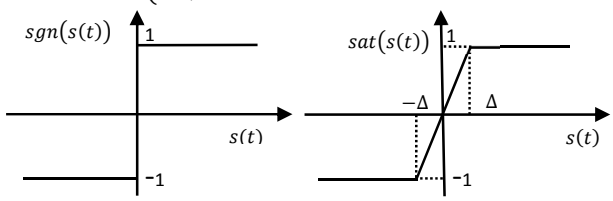

(a) (b)

Fig. 2. Plot of (a) $sgn\big(s(t)\big)$ and (b) $sat\big(s(t)\big)$ functions

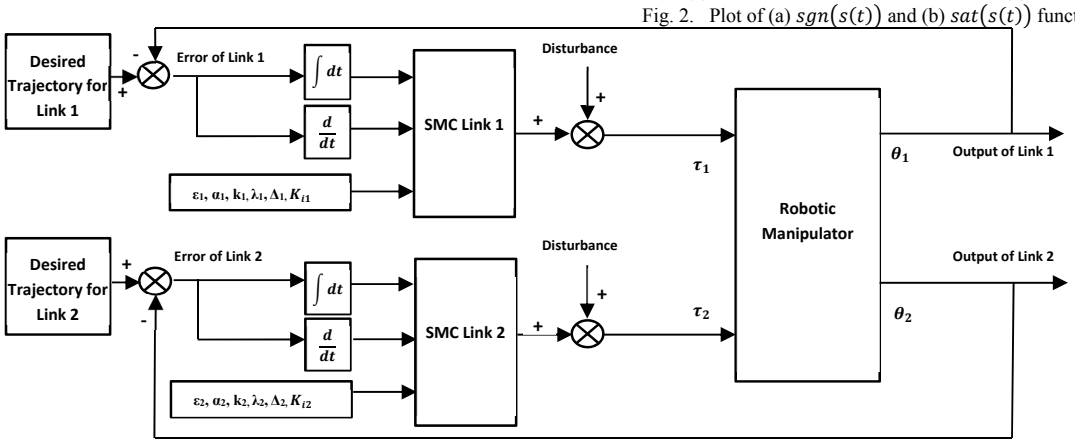

Fig. 3. Block Diagram of Two-link Manipulator with SMCPID

Lyapunov stability is described for two-link robotic manipulator with SMC, where Lyapunov function is taken as:

$$\dot{V}(t) = s(t)\dot{s}(t) \quad (10)$$

Necessary condition for a stable system is:

$$\dot{V}(t) \leq -\eta|s(t)|, \text{ where } \eta > 0 \quad (11)$$

where η is a constant and $V(t)$ is Lyapunov surface, such that $V(t) = {}^{1}/_{2}\left(s(t)\right)^2$. Considering (6), (7) and (8), it can be proved that all the three reaching control laws suffice the condition as described in (11).

Dynamic equations with modified controller output are obtained for three reaching laws.

Equation (12) describes the modified controller output when constant rate law is used.

$$\tau = M(\theta)\left(\lambda\,\dot{e}(t) + \varepsilon\, sat\left(s(t)\right) + \ddot{\theta}_d + k_i e(t)\right) + C\left(\theta, \dot{\theta}\right) + G(\theta) \quad (12)$$

As seen from (7), modified controller output, (13) is derived for exponential reaching law.

$$\tau = M(\theta)\left(\lambda\,\dot{e}(t) + \varepsilon\, sat\left(s(t)\right) + ks(t) + \ddot{\theta}_d + k_i e(t)\right) + C\left(\theta, \dot{\theta}\right) + G(\theta) \quad (13)$$

Similarly for power rate reaching law, (14) describes controller output for two-link planar rigid robotic manipulator.

$$\tau = M(\theta)\left(\lambda\,\dot{e}(t) + k|s(t)|^{\alpha}\, sat\left(s(t)\right) + \ddot{\theta}_d + k_i e(t)\right) + C\left(\theta, \dot{\theta}\right) + G(\theta) \quad (14)$$

All the gains as described in (12), (13), and (14), such as λ, ε, k and α are required to be tuned, to reduce the tracking error and chattering in controller output, for the optimum performance of robotic manipulator.

IV. Simulations and Results

MATLAB (R2014a) was used for simulation of dynamic model (12), (13), and (14) with fourth order Runge-Kutta method. Sampling time and torque constraints were taken as 1ms and [-20 20] N-m for both links, respectively. Genetic Algorithm (GA) was used to tune SMC gain parameters. Range for ε, k and λ for optimisation was taken from 1 to 1000, and for α and Δ, it was from 0 to1. Generations and population size were taken as 100 and 50, respectively. Function tolerance was set as 1E-06.

The fitness function was designed to obtain two objectives, which are minimisation of sum integral absolute error (IAE) of both links and reduction of chattering.

$$IAE = \int_0^t \{|e_1| + |e_2|\}dt \quad (15)$$

here e_1 and e_2 are the errors of link 1 and link 2 respectively. Objective of IAE is to minimize tracking error in both links.

$$chatter = \int_0^t \{|s_1| + |s_2|\}dt \quad (16)$$

where s_1 and s_2 are surface errors of both links. Objective of (16) is to reduce chattering in the controller output [13].

$$O(n) = [W_1(IAE) + W_2(chatter)] \quad (17)$$

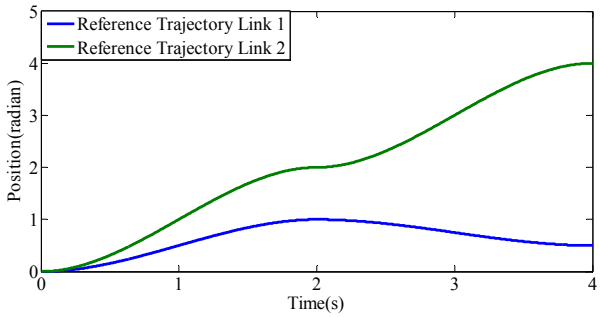

Fig. 4. Reference/Desired Trajectories for link 1 and link 2

Equation (17) describes fitness function which simultaneously fulfils both the objectives. W_1 and W_2 are taken as 0.999 and 0.001 to make values of IAE and $chatter$ comparable.

Desired trajectories to be tracked for link 1 and link 2 are given by (18) and (19) [9].

$$\theta_{d1}(t) = \begin{cases} 0.75t^2 - 0.25t^3, & 0 \leq t \leq 2 \\ -1.5 + 3t - 1.125t^2 + 0.125t^3, & 2 \leq t \leq 4 \end{cases} \quad (18)$$

$$\theta_{d2}(t) = \begin{cases} 1.5t^2 - 0.5t^3, & 0 \leq t \leq 2 \\ 12 - 12t + 4.5t^2 - 0.5t^3, & 2 \leq t \leq 4 \end{cases} \quad (19)$$

where $\theta_{d1}(t)$ and $\theta_{d2}(t)$ are the desired trajectories for link 1 and link 2, respectively. The other required parameters are set as $\theta_{d1}(t) = 1$ radian and $\theta_{d2}(t) = 2$ radian at $t = 2\,s$, $\theta_{d1}(t) = 0.5$ radian and $\theta_{d2}(t) = 4$ radian at $t = 4\,s$ and $\dot{\theta}_{d1}(t) = \dot{\theta}_{d2}(t) = 0$ at $t = 2\,s$ and $4\,s$. Fig. 4 shows the reference trajectories of respective links as described by (18) and (19).

A. Trajectory tracking

Values of tuned parameters of SMCPID for two-link planar rigid robotic manipulator are shown in Table II, whereas trajectory tracking for link 1 and link 2 are shown in Figs. 5 and 6, respectively. IAE and chatter of respective links, and fitness function values are shown in Table III. As seen graphically in Fig. 7, IAE values for constant rate, exponential and power rate reaching laws have marginal difference, thus it can be concluded that all the three laws performed equally well in terms of trajectory tracking.

TABLE II. TUNED PARAMETERS

SMCPID reaching laws		*Parameters*					
		ε	***k***	***α***	***λ***	***Δ***	k_i
Link 1	Constant rate	875.9	-	-	937.51	0.47	968.32
	Exponential	732.34	578.79	-	736.89	0.5	981.81
	Power rate	-	984.86	0.04	682.91	0.38	796.29
Link 2	Constant rate	571.62	-	-	925.3	0.31	950.2
	Exponential	818.96	951.94	-	909.83	0.88	967.36
	Power rate	-	852.97	0.02	999.49	0.37	943.74

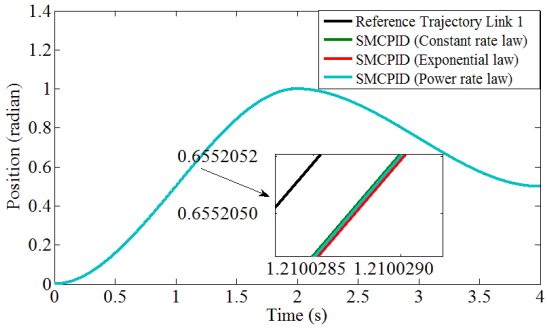

Fig. 5. Trajectory tracking for link 1

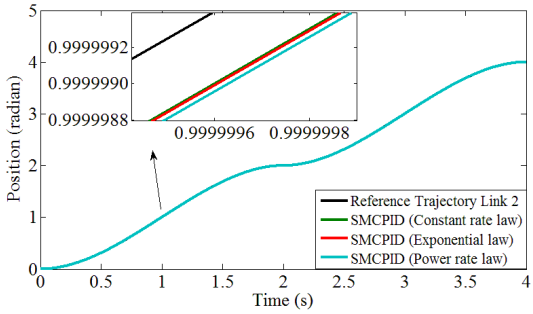

Fig. 6. Trajectory tracking for link 2

TABLE III. OPTIMIZED IAE, CHATTER AND FITNESS FUNCTION

SMCPID reaching laws	*IAE*		*Chatter*		*Fitness Function*
	Link 1	*Link 2*	*Link 1*	*Link 2*	
Constant rate law	1.02E-06	2.73E-06	6.32E-04	1.71E-03	6.09E-06
Exponential law	1.05E-06	2.75E-06	5.92E-04	1.67E-03	6.06E-06
Power rate law	1.02E-06	2.83E-06	6.42E-04	1.63E-03	6.13E-06

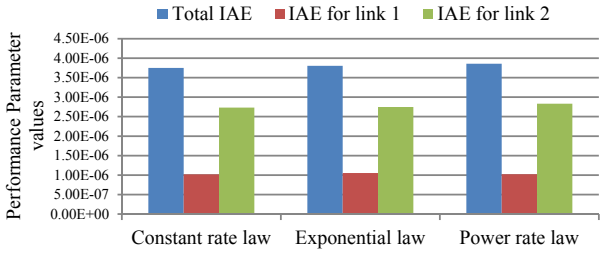

Fig. 7. Comparison of parameters of SMCPID reaching laws

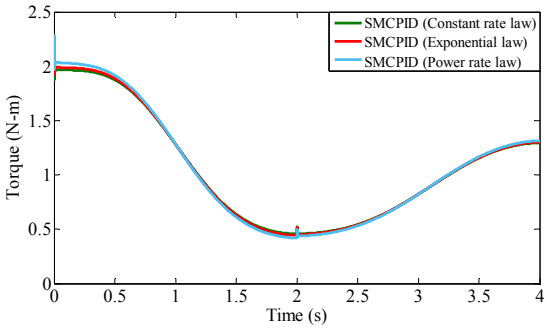

Fig. 8. Controller output for link 1

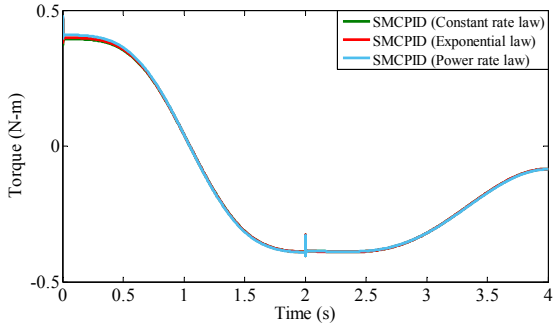

Fig. 9. Controller output for link 2

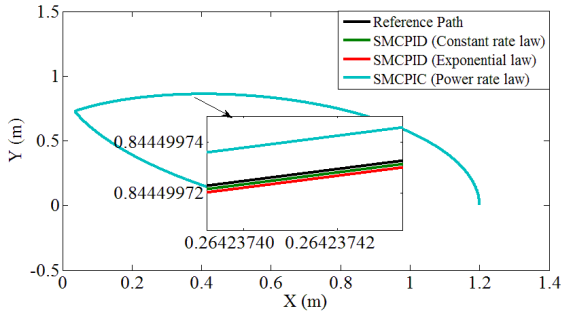

Fig. 10. Path tracked by end-effector

Figs. 8, 9, and 10 show the controller output for link 1 and link 2, and path tracked by end-effector in X and Y plane, respectively.

B. *Disturbance Rejection*

To investigate the capability of the controller, disturbance rejection study plays a key role. Three case studies were investigated for disturbance rejection. A disturbance of A(sin(50t)) is applied one by one to link 1, link 2 and both links of the robotic manipulator, where A varies from 1.0 to 1.9. Table IV describes the fitness function values for disturbances injected in controller output. A typical case for is considered when value of 'A' is taken as 1.9, hence disturbance of 1.9(sin(50t)) is applied to torque input of the robotic manipulator. For this case, plot for trajectory tracking, controller output for link 1 and link 2, and path tracked by end-effector are shown in Figs. 11, 12, 13, 14 and 15, respectively. Also, fig. 16 shows the variation of fitness graphically. From Table IV and Fig. 16, it can be clearly observed that power rate reaching law performed better than other reaching laws.

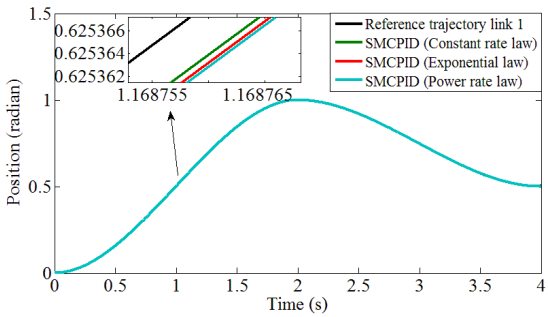

Fig. 11. Trajectory tracking of link 1 for Disturbance of 1.9sin50t

TABLE IV. FITNESS FUNCTION VALUES FOR DISTURBANCE

Disturbance	*Disturbance in link 1*			*Disturbance in link 2*			*Disturbance in both links*		
	Fitness function values (×1E-05)			*Fitness function values (×1E-04)*			*Fitness function values (×1E-04)*		
	Constant rate law	*Exponential law*	*Power rate law*	*Constant rate law*	*Exponential law*	*Power rate law*	*Constant rate law*	*Exponential law*	*Power rate law*
1.0sin(50t)	7.66	7.67	7.61	3.14	3.13	2.96	2.96	2.95	2.81
1.1sin(50t)	8.34	8.42	8.33	3.46	3.44	3.25	3.26	3.25	3.08
1.2sin(50t)	9.08	9.17	9.05	3.77	3.75	3.54	3.56	3.54	3.36
1.3sin(50t)	9.82	9.92	9.77	4.08	4.06	3.82	3.85	3.84	3.63
1.4sin(50t)	10.56	10.67	10.49	4.40	4.37	4.11	4.15	4.13	3.90
1.5sin(50t)	11.30	11.42	11.20	4.71	4.69	4.40	4.44	4.43	4.17
1.6sin(50t)	12.05	12.17	11.92	5.02	5.00	4.68	4.74	4.72	4.44
1.7sin(50t)	12.79	12.92	12.63	5.34	5.31	4.97	5.04	5.02	4.71
1.8sin(50t)	13.54	13.67	13.35	5.65	5.62	5.25	5.33	5.31	4.99
1.9sin(50t)	14.28	14.42	14.06	5.97	5.94	5.54	5.63	5.61	5.26

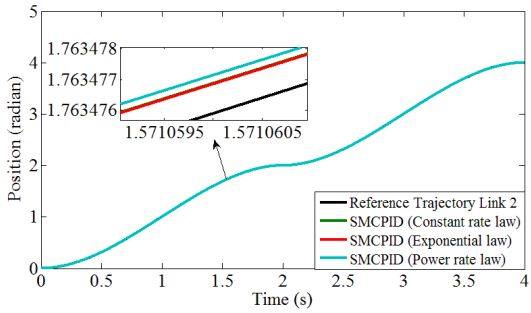

Fig. 12. Trajectory tracking of link 2 for Disturbance of 1.9sin50t

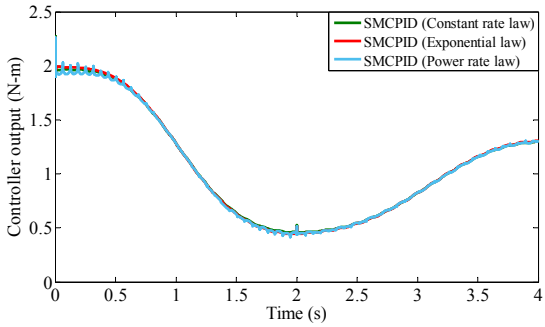

Fig. 13. Controller output of link 1 for Disturbance of 1.9sin50t

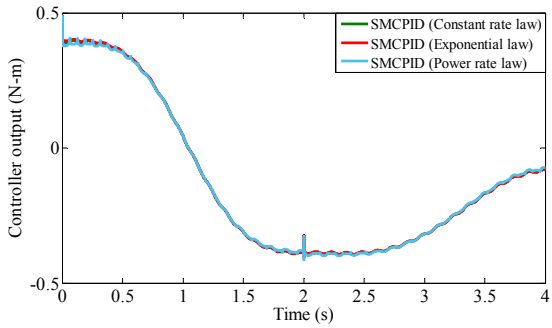

Fig. 14. Controller output of link 2 for Disturbance of 1.9sin50t

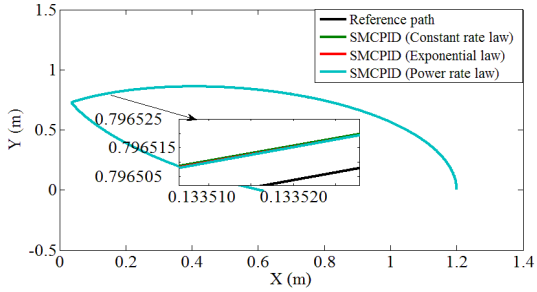

Fig. 15. Path tracked by end-effector for Disturbance of 1.9sin50t

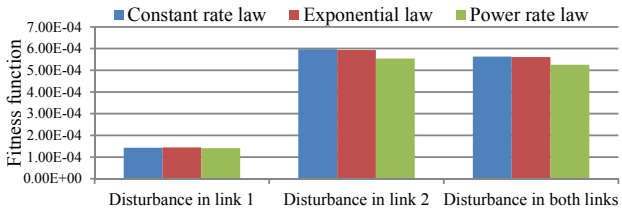

Fig. 16. Variation in fitness function value for a disturbance of 1.9sin(50t) in controller output

C. *Uncertainty in mass*

Uncertainty test was performed by changing the dynamic mass of end-effector. Four cases were considered where mass of link 2 changes from (a) 0.5 kg to 0.1 kg, (b) 0.4 kg to 0.1 kg, (c) 0.3 kg to 0.1 kg, and (d) 0.2 kg to 0.1 kg with respect to time and their respective fitness function values are as shown in Table V. Profile for change in mass was designed for the uncertainty test as shown in Fig. 17.

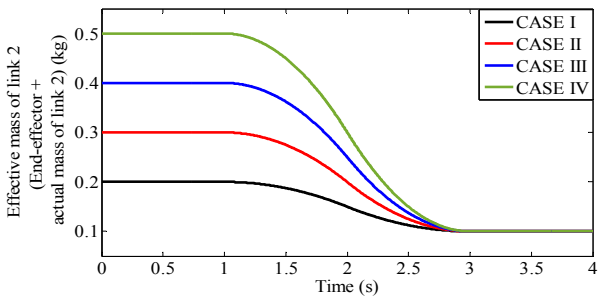

Fig. 17. Profile for change in mass of end-effector

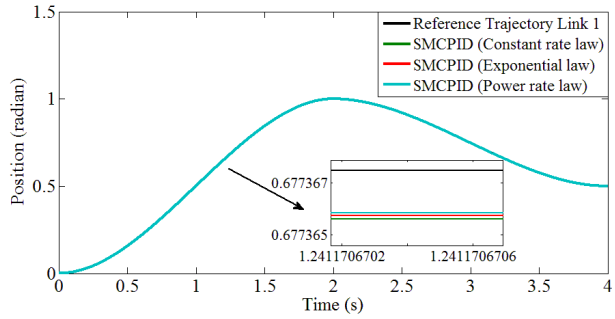

Fig. 18. Trajectory tracking for link 1 when CASE IV is considered.

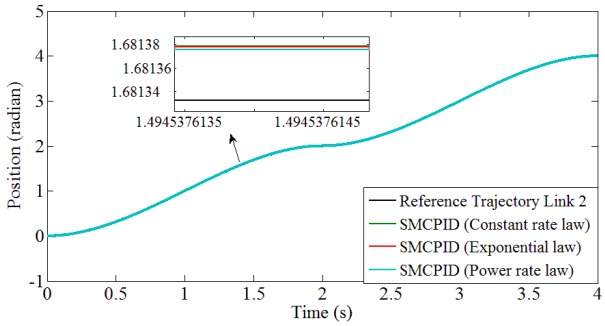

Fig. 19. Trajectory tracking for link 2 when CASE IV is considered.

TABLE V. FITNESS FUNCTION VALUES FOR MASS CHANGE UNCERTAINITY TEST

Mass of End Effector (kg)		*Fitness function values (×1E-05)*		
		Constant rate law	*Exponential law*	*Power rate law*
Case I	0.1	5.04E-05	4.96E-05	4.76E-05
Case II	0.2	9.90E-05	9.75E-05	9.23E-05
Case III	0.3	1.48E-04	1.45E-04	1.36E-04
Case IV	0.4	1.96E-04	1.93E-04	1.80E-04

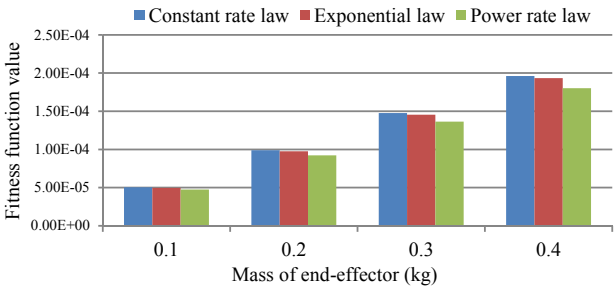

Fig. 20. Comparison of fitness function for mass uncertainity test

Trajectory tracking for the two links are shown in Fig. 18 and 19, respectively for the case when mass of end effector is considered as 0.4 (Case IV, with reference to Table V).

It can be seen from Table V and graphically by Fig. 20 that power rate reaching law performed better with respect to other two reaching laws.

V. CONCLUSIONS

Proportional, Integral and Derivative (PID) type surface variation of sliding mode control (SMC) is investigated for constant rate, exponential and power rate reaching laws applied to a two-link planar robotic manipulator. Genetic Algorithm based tuning technique was used to tune the parameters of SMC to achieve two objectives i.e. minimum Integral Absolute Error (IAE) in trajectory tracking and minimum chattering in the controller output. Trajectory tracking performance showed that all the three reaching laws performed equally in terms of IAE, while disturbance rejection and mass uncertainty tests revealed that power rate reaching offered significantly better performance than the other two laws. A decrease in fitness function value by approximately 6.23% from exponential law and 6.57% from constant rate law was reported as compared to power rate law when a disturbance of 1.9sin(50t) was injected in the controller output of both links of robotic manipulator. Furthermore, a typical case IV in mass uncertainty test showed that power rate law gave approximately 6.73% and 8.13% better fitness function values with respect to exponential law and constant rate law, respectively. A similar trend was observed in other three cases.

REFERENCES

[1] Acob, J.M., Pano, V. and Ouyang, P.R. (2013), "Hybrid PD Sliding Mode Control of a Two Degree of-freedom Parallel Robotic Manipulator", *IEEE International Conference on Control and Automation (ICCA)*, pp. 1760–1765, June 2013.

[2] Fallaha, C.J., Saad, M., Kanaan, H.Y. and Al-Haddad, K. (2011), "Slidingmode Robot Control with Exponential Reaching Law", *IEEE Transactions on Industrial Electronics*, Vol. 58, pp. 600–610, February 2011.

[3] Kuo, T.C., Huang, Y.J. (2005), "A Sliding Mode PID-Controller Design for Robotic Manipulators", *International Symposium on Computational Intelligence in Robotics and Automation (ISCIRA)*, IEEE, pp. 625–629.

[4] Vyas, D., Ohri, J. and Patel, A. (2013), "Comparison of Conventional & Fuzzy based Sliding Mode PID Controller for Robot Manipulator", *International Conference on Individual and Collective Behaviors in Robotics (ICICBR)*, IEEE , pp. 115–119.

[5] Vijay, M. and Jena, D. (2014), "Optimal GA based SMC with Adaptive PID Sliding Surface for Robot Manipulator", *International Conference on Industrial and Information Systems (ICIIS)*, IEEE, pp. 1–6.

[6] Chen, W.D., Wang, H.T., Tang, D.Z. and Wang, H.R. (2003), "Fuzzy Slidingmode Control based on State for Robotic Manipulators", *International Conference on Machine Learning and Cybernetics*, IEEE, Vol. 2, pp. 957–960, November 2003.

[7] Craig, J.J. (2005), *Introduction to Robotics-Mechanics and Control*, Pearson Prentice Hall.

[8] Niku, S.B. (2012), *Introduction to Robotics-Analysis, Control, Applications*, Wiley, pp. 151–154.

[9] Ayala, H.V.H. and Coelho, L.D.S. (2012), "Tuning of PID Controller based on a Multiobjective Genetic Algorithm Applied to a Robotic Manipulator", *Expert Systems with Applications*, Elsevier, pp. 8968–8974.

[10] Sharma, R., Rana, K.P.S. and Kumar, V. (2014), "Performance Analysis of Fractional Order Fuzzy PID Controllers Applied to a Robotic Manipulator", *Expert Systems with Applications*, Elsevier, pp. 4274–4289.

[11] Young, K.D., Utkin, V.I. and Ozguner, U. (1999), "A Control Engineer's Guide to Sliding Mode Control", *IEEE Transactions on Control Systems Technology*, Vol. 7, pp. 328–342, May 1999.

[12] Liu, J. and Wang, X. (2012), *Advanced Sliding Mode Control for Mechanical Systems*, Springer, 2012.

[13] Delavari, H., Ghaderi, R., Ranjbar, A. and Momani, S. (2010), "Fuzzy Fractional Order Sliding Mode Controller for Nonlinear Systems", *Commun Nonlinear Sci. Numer Simulat*, Elsevier, pp. 963–978.